

# Self-triggered Feedback Control Systems with Finite-Gain $\mathcal{L}_2$ Stability

Xiaofeng Wang and M.D. Lemmon

## Abstract

This paper examines a class of real-time control systems in which each control task triggers its next release based on the value of the last sampled state. Prior work [1] used simulations to demonstrate that self-triggered control systems can be remarkably robust to task delay. This paper derives bounds on a task's sampling period and deadline to quantify how robust the control system's performance will be to variations in these parameters. In particular we establish inequality constraints on a control task's period and deadline whose satisfaction ensures that the closed loop system's induced  $\mathcal{L}_2$  gain lies below a specified performance threshold. The results apply to linear time-invariant systems driven by external disturbances whose magnitude is bounded by a linear function of the system state's norm. The plant is regulated by a full-information  $\mathcal{H}_\infty$  controller. These results can serve as the basis for the design of soft real-time systems that guarantee closed-loop control system performance at levels traditionally seen in hard real-time systems.

## I. INTRODUCTION

Computer-controlled systems are often implemented using periodic tasks satisfying hard real-time constraints. Under a periodic task model, consecutive invocations (also called jobs) of a task are released in a periodic manner. If the task model satisfies a hard real-time constraint, then each job completes its execution by a specified deadline. Hard real-time periodic task models allow the control system designer to treat the computer-controlled system as a discrete-time system, for which there are a variety of mature controller synthesis methods.

Both authors are with the department of electrical engineering, University of Notre Dame, Notre Dame, IN 46556; e-mail: xwang13,lemmon@nd.edu. The authors gratefully acknowledge the partial financial support of the National Science Foundation (grants NSF-ECS-0400479 and NSF-CNS-0410771)

Periodic task models may be undesirable in many situations. Traditional approaches for estimating task periods and deadlines are very conservative, so the control task may have greater utilization than it actually needs. This results in significant over-provisioning of the real-time system hardware. With such high utilization, it may be difficult to schedule other tasks on the same processing system. Finally, it should be noted that real-time scheduling over networked systems may be poorly served by the periodic task model. In many networked systems, tasks are finished only after information has been successfully transported across the network. It is often unreasonable to expect hard real-time guarantees on message delivery in communication networks. This is particularly true for wireless sensor-actuator networks. In these applications, there may be good reasons to consider alternatives to periodic task models.

This paper considers a **self-triggered** task model in which each task determines the release of its next job. In reality, one might consider periodic task models as self-triggered tasks since many implementations release tasks upon expiration of a one-shot timer that was started by the previous invocation of the task. Under a periodic task model, the period of this one-shot timer is always a constant value. This paper, however, considers a more adaptive form of self-triggering in which the value loaded into the one-shot timer is actually a function of the system state sampled by the current job. Under this “state-based” self-triggering, each task releases its next job based on the system state. We can therefore consider “state-based” self-triggering as a closed-loop form of releasing tasks for execution, whereas periodic task models release their jobs in an open-loop fashion. For simplicity, this paper refers to a “state-based” self-triggered task model as “self-triggered”.

Self-triggering provides a more flexible way of adjusting task periods. Since task periods are based on the system’s current state, it is possible to reduce control task utilization during periods of time when the system is sitting happily at its equilibrium point. The question here is precisely how much freedom do we have in adjusting task periods in response to variations in the system state. This paper answers that question by providing bounds on the task periods and deadlines required to assure a specified level of  $\mathcal{L}_2$  stability. Our results pertain to linear time-invariant system with state feedback. Since our controller seeks to ensure  $\mathcal{L}_2$  stability, we use a full-information  $\mathcal{H}_\infty$  controller in our analysis. We also assume that the system has a process noise whose magnitude is bounded by a linear function of the norm of the system state. Under these assumptions we obtain a set of inequality constraints on the task period and deadlines as a

function of the system state. On the basis of simulation results, these bounds appear to be tight and relatively easy to compute, so it may be possible to use them in actual real-time control systems.

The remainder of this paper is organized as follows. Section II discusses the prior work related to self-triggered feedback. Section III introduces the system model. Section IV derives sufficient threshold condition that can serve as an event triggering state sampling. In section V, the self-triggering scheme is presented and the system is shown to be  $\mathcal{L}_2$  stable. Simulations are shown in section VI. Finally, conclusions and future work are presented in section VII.

## II. PRIOR WORK

To the best of our knowledge there is relatively little prior work examining state-based self-triggered feedback control. A self-triggered task model was introduced by Velasco et al. [2] in which a heuristic rule was used to adjust task periods. A self-triggered task model was also introduced by Lemmon et al. [1] which chose task periods based on a Lyapunov-based technique. But other than these two papers, we are aware of no other serious work looking at self-triggered feedback schemes. There is, however, a great deal of related work dealing with so-called event-triggered feedback, sample period selection, and real-time control system co-design. We'll review each of these areas in more detail below and then discuss their relationship to the self-triggered task models.

Traditional methods for sample period selection [3] are usually based on Nyquist sampling. Nyquist sampling ensures that the sampled signal can be perfectly reconstructed from its samples. In practice, however, feedback within the control system means the system's performance will be somewhat insensitive to errors in the feedback signal, so that perfect reconstruction is much more than we require in a feedback control system. An alternative approach to the sample period selection problem makes use of Lyapunov techniques. This was done in Zheng et al. [4] for a class of nonlinear sampled-data system. Nesic et al. [5] used input-to-state stability (ISS) techniques to bound the inter-sample behavior of nonlinear systems. The sample periods obtained by these methods also tend to be very conservative due to the bounding techniques used.

The prior work on sample-period selection using Lyapunov methods can determine sampling periods ensuring asymptotic stability in nonlinear systems. For the linear systems we consider,

these methods can yield very tight estimates on the sampling period. This was actually demonstrated by Tabuada et al. [6] and the basic technique employed by Tabuada to estimate sample periods is used in this paper as well.

Another related research direction viewed sample period selection as a “co-design” problem that involves both the control system and the real-time system. In this case, sample periods are selected to minimize some penalty on control system performance subject to a schedulability condition. Early statements of this problem may be found in Seto et al. [7] with more recent studies in [8] and [9]. The penalty function is often a performance index for an infinite horizon optimal control problem. It has, however, been demonstrated [10] that such indices are rarely monotone functions of the sampling period. As a result, it only appears to be feasible to do off-line determination of these “optimal” sampling periods.

The prior work on co-design really focuses on optimizing performance subject to scheduling constraints. The scheduling constraints are Liu-Layland [11] schedulability conditions for earliest deadline first (EDF) scheduling. It is not always clear, however, that these are the best set of constraints to be using. This paper actually derives a set of constraints on both the periods and deadlines that we can then use as a quality-of-service (QoS) constraint that the real-time scheduler needs to meet. We do not address the schedulability of these QoS constraints in this paper, though that is an important research issue that we are still studying.

In recent years, a number of researchers have proposed aperiodic and sporadic task models in which tasks are event-triggered [12]. By event-triggering, we usually mean that the system state is sampled when some function of the system state exceeds a threshold. The idea of event-triggered feedback has appeared under a variety of names, such as interrupt-based feedback [13], Lebesgue sampling [14], asynchronous sampling [15], or state-triggered feedback [6]. Event triggering usually requires some form of hardware event detector to generate a hardware interrupt to release the control task. This can be done using either custom analog integrated circuits (ASIC's) or floating point gate array (FPGA) processors.

The prior work on event-triggered feedback is probably most closely related to this paper's work. In particular, the bounds we derive in this paper are based on variations of the event-triggering conditions used by Tabuada et al. [6]. The conditions given in our paper appear to be less conservative than the bounds obtained in [6].

### III. SYSTEM MODEL

Consider a linear time-invariant system whose state  $x : \mathfrak{R} \rightarrow \mathfrak{R}^n$  satisfies the initial value problem,

$$\begin{aligned}\dot{x}(t) &= Ax(t) + Bu(t) + w(t) \\ x(0) &= x_0\end{aligned}$$

where  $u : \mathfrak{R} \rightarrow \mathfrak{R}^m$  is a control input and  $w : \mathfrak{R} \rightarrow \mathfrak{R}^n$  is an exogenous disturbance function in  $\mathcal{L}_2$  such that there exists a positive real constant  $W > 0$  so that  $\|w(t)\|_2 \leq W\|x(t)\|_2$  for all  $t \geq 0$ . In the above equation,  $A \in \mathfrak{R}^{n \times n}$  and  $B \in \mathfrak{R}^{n \times m}$  are real matrices of appropriate dimensions.

Since we're interested in controllers that are finite-gain  $\mathcal{L}_2$  stable, we assume there exists a full-information  $\mathcal{H}_\infty$  controller that asymptotically stabilizes the unforced system. In particular, we assume there exists a symmetric positive definite matrix  $P$  such that

$$\dot{x}(t) = (A - BB^T P)x(t) \tag{1}$$

has an asymptotically stable equilibrium. The matrix  $P$  satisfies the  $\mathcal{H}_\infty$  algebraic Riccati equation (ARE),

$$0 = PA + A^T P - Q + R \tag{2}$$

where

$$Q = PBB^T P \tag{3}$$

$$R = I + \frac{1}{\gamma^2} PP \tag{4}$$

for some real constant  $\gamma > 0$ . For notational convenience the system matrix of the closed loop system (equation 1) will be denoted as  $A_{cl} = A - BB^T P$ . The state feedback gain matrix is  $K = -B^T P$ .

If we consider the standard  $\mathcal{L}_2$  storage function  $V : \mathfrak{R}^n \rightarrow \mathfrak{R}$  given by  $V(x) = x^T P x$  for all  $x \in \mathfrak{R}^n$  then the preceding assumptions about  $P$  allow us to show that the storage function's directional derivative satisfies the dissipative inequality,

$$\dot{V}(x(t)) < -\|x(t)\|_2^2 + \gamma^2 \|w(t)\|_2^2 \tag{5}$$

for all  $t$ . Recall that a linear system,  $T$ , is said to be finite gain  $\mathcal{L}_2$  stable if  $T$  is a linear operator from  $\mathcal{L}_2$  back into  $\mathcal{L}_2$ . The induced gain of  $T$  is

$$\|T\| = \sup_{\|w\|_{\mathcal{L}_2}=1} \|Tw\|_{\mathcal{L}_2}.$$

Satisfaction of the dissipative inequality (eq. 5) is sufficient to show that the system  $T$  characterized by the state equation

$$\dot{x}(t) = (A - BB^T P)x(t) + w(t) \quad (6)$$

is finite gain  $\mathcal{L}_2$  stable with an induced gain less than  $\gamma$ .

This paper considers a sampled-data implementation of the closed loop system in equation 6. This means that the plant's control,  $u$ , is computed by a computer task. This task is characterized by two monotone increasing sequences of time instants; the release time sequence  $\{r_k\}_{k=0}^{\infty}$  and the finishing time sequence  $\{f_k\}_{k=0}^{\infty}$ . We say these two sequences are admissible if  $r_k \leq f_k < r_{k+1}$  for all  $k = 0, \dots, \infty$ . The time  $r_k$  denotes the time when the  $k$ th invocation of a control task (also called a job) is released for execution on the computer's central processing unit (CPU). At this time, we assume that the system state is sampled so that  $r_k$  also represents the  $k$ th sampling time instant. The time  $f_k$  denotes the time when the  $k$ th job has finished executing. Each job of the control task computes the control  $u$  based on the last sampled state. Upon finishing, the control job outputs this control to the plant. The control signal used by the plant is held constant by a zero-order hold (ZOH) until the next finishing time  $f_{k+1}$ . This means that the sampled-data system under study in this project satisfies the following set of state equations,

$$\begin{aligned} \dot{x}(t) &= Ax(t) + Bu(t) + w(t) \\ u(t) &= -B^T Px(r_k) \end{aligned} \quad (7)$$

for  $t \in [f_k, f_{k+1})$  and all  $k = 0, \dots, \infty$ . The state trajectories  $x$  satisfying equation 7 are continuous so that the initial state at time  $f_k$  is simply  $x(f_k) = \lim_{t \uparrow f_k} x(t)$ .

We let  $T_k = r_{k+1} - r_k$  denote the  $k$ th inter-release time ( $k = 0, \dots, \infty$ ).  $T_k$  can therefore be interpreted as a time-varying ‘‘sampling’’ period by control engineers and a time-varying ‘‘task’’ period by real-time system engineers. We let  $D_k = f_k - r_k$  denote the time interval between the  $k$ th job's release and finishing time. Control engineers would view  $D_k$  as the ‘‘delay’’ of the  $k$ th job whereas real-time system engineers would view  $D_k$  as the ‘‘jitter’’ of the  $k$ th job. If the

control task satisfies a hard real-time constraint, then the delay  $D_k$  is required to lie below a specified “deadline”.

If we decrease the sampling period,  $T_k$ , and delay,  $D_k$ , in a uniform manner so that the resulting release and finishing time sequences remain admissible, then the state trajectories generated by the sampled-data system in equation 7 will converge to state trajectories satisfying the original closed-loop system equation 6. By construction of the control, we know that this original system is  $\mathcal{L}_2$  stable with gain less than  $\gamma$ . This paper’s main results establish nontrivial bounds on the sequence of sampling periods  $\{T_k\}_{k=0}^{\infty}$  and delays  $\{D_k\}_{k=0}^{\infty}$  such that the resulting release and finishing time sequences are admissible and the sampled-data system preserves the original system’s  $\mathcal{L}_2$  stability.

#### IV. $\mathcal{L}_2$ STABILITY

Consider the sampled-data system in equation 7 with a set of admissible release and finishing time sequences. For all  $k$ , define the  $k$ th job’s error function  $e_k : [r_k, f_{k+1}) \rightarrow \mathfrak{R}^n$  by  $e_k(t) = x(t) - x(r_k)$ . This error represents the difference between the current system state and the system state at the last release time,  $r_k$ . This section presents two inequality constraints on  $e_k(t)$  (see theorem 4.1 and corollary 4.2 below) whose satisfaction is sufficient to ensure that the sampled-data system’s  $\mathcal{L}_2$  gain is less than  $\gamma/\beta$  for some parameter  $\beta \in (0, 1]$ .

**Notational conventions:** The sufficient conditions derived in this section apply uniformly to all jobs,  $k$ . We may therefore, for notational convenience, drop the job index  $k$  with the understanding that we’re only considering the  $k$ th job’s error signal. In particular, the times  $r_{k-1}$ ,  $r_k$ ,  $r_{k+1}$ ,  $f_k$ , and  $f_{k+1}$  will be denoted as  $r^-$ ,  $r$ ,  $r^+$ ,  $f$ , and  $f^+$ , respectively. The system state at time  $t \in [r_k, f_{k+1})$  will be denoted as  $x_t$  and the  $k$ th job’s error signal,  $e_k(t)$ , at time  $t$  will be denoted as  $e_t = x_t - x_r$  for  $t \in [r, f^+)$ .

The following theorem states that if a function of the state error  $e_k(t)$  and state  $x(t)$  satisfies a certain inequality constraint, then the closed loop system in equation 7 is finite gain  $\mathcal{L}_2$  stable.

*Theorem 4.1:* Consider the sampled-data system in equation 7 with admissible release and finishing time sequences. Let  $\beta$  be any real constant in the open interval  $(0, 1)$  with the matrix  $Q$  as given in equation 3. If

$$e_k^T(t)Qe_k(t) < (1 - \beta^2)\|x(t)\|_2^2 + x_r^T Qx_r \quad (8)$$

for all  $t \in [f_k, f_{k+1})$  and any  $k = 0, \dots, \infty$ , then the sampled-data system is finite gain  $\mathcal{L}_2$  stable with a gain less than  $\gamma/\beta$ .

*Proof:* Consider the storage function  $V : \mathfrak{X}^n \rightarrow \mathfrak{R}$  given by  $V(x) = x^T P x$  for  $x \in \mathfrak{X}^n$  where  $P$  is a symmetric positive definite matrix satisfying the algebraic Riccati equation (eq. 2). The directional derivative of  $V$  for  $t \in [f_k, f_{k+1})$  is

$$\begin{aligned} \dot{V} &= \frac{\partial V}{\partial x} (Ax_t - BB^T P x_r + w) \\ &= -x_t^T \left( I - Q + \frac{1}{\gamma^2} P P \right) x_t - 2x(t)^T Q x_r + 2x_t^T P w \\ &= -x_t^T (I - Q) x_t - \left\| \gamma w_t - \frac{1}{\gamma} P x_t \right\|_2^2 + \gamma^2 \|w_t\|_2^2 - 2x_t^T Q x_r \\ &\leq -x_t^T (I - Q) x_t + \gamma^2 \|w_t\|_2^2 - 2x_t^T Q x_r \end{aligned} \quad (9)$$

Insert  $x_t = e_t + x_r$  into the above equation to obtain

$$\begin{aligned} \dot{V} &\leq -\|x_t\|_2^2 + [e_t + x_r]^T Q [e_t + x_r] - 2[e_t + x_r]^T Q x_r + \gamma^2 \|w_t\|_2^2 \\ &= -\|x_t\|_2^2 + e_t^T Q e_t - x_r^T Q x_r + \gamma^2 \|w_t\|_2^2 \end{aligned} \quad (10)$$

By the assumption in equation 8, we know that equation 10 can be rewritten as

$$\dot{V} \leq -\beta^2 \|x_t\|_2^2 + \gamma^2 \|w_t\|_2^2 \quad (11)$$

This is the dissipative inequality that holds for all  $t$  and is sufficient to ensure the sampled-data system is  $\mathcal{L}_2$  stable with a gain less than  $\gamma/\beta$ . ■

In our following work, we'll find it convenient to use a slightly weaker sufficient condition for  $\mathcal{L}_2$  stability which is only a function of the state error  $e_k(t)$ . The following corollary states this result.

*Corollary 4.2:* Consider the sampled-data system in equation 7 with admissible sequences of release and finishing times. Let  $Q$  be a real matrix that satisfies equation 3 and  $\beta$  be a real constant in the interval  $(0, 1]$  such that the matrix

$$M = (1 - \beta^2)I + Q. \quad (12)$$

has full rank. If the state error trajectory satisfies

$$e_k(t)^T M e_k(t) \leq x_r^T M x_r \quad (13)$$



for  $t \in [f_k, f_{k+1})$  for all  $k = 0, \dots, \infty$ , then the sampled data system is  $\mathcal{L}_2$  stable with a gain less than  $\gamma/\beta$ .

*Proof:* Equation 13 can be rewritten as

$$\begin{aligned} e_k(t)^T M e_k(t) &= (1 - \beta^2) \|e_k(t)\|_2^2 + e_k(t)^T Q e_k(t) \\ &\leq (1 - \beta^2) \|x_r\|_2^2 + x_r^T Q x_r \end{aligned}$$

This can be rewritten to obtain

$$\begin{aligned} e_k(t)^T Q e_k(t) &\leq (1 - \beta^2) (\|x_r\|_2^2 - \|e_k(t)\|_2^2) + x_r^T Q x_r \\ &\leq (1 - \beta^2) \|x(t)\|_2^2 + x_r^T Q x_r \end{aligned}$$

where we used the fact that

$$\|x_r\|_2^2 - \|e_t\|_2^2 \leq \|x_r + e_t\|_2^2 = \|x(t)\|_2^2.$$

This inequality is the sufficient condition in theorem 4.1 so we can conclude that the sampled-data system is  $\mathcal{L}_2$  stable with a gain less than  $\gamma/\beta$ . ■

*Remark 4.3:* The inequalities in equations 8 or 13 can both be used as the basis for an event-triggered feedback control system (section II). Note that both inequalities are trivially satisfied at  $t = r_k$ . If we let the delay,  $D_k$ , be zero for each job, then by triggering the release times  $\{r_k\}_{k=0}^{\infty}$  anytime before the inequalities in equations 8 or 13 are violated, we will ensure the sampled-data system's induced  $\mathcal{L}_2$  gain remains below  $\gamma/\beta$ . The resulting event-triggered feedback system is very similar to the state-triggering scheme proposed by Tabuada et al. [6] for asymptotic stability. The main difference between that result and this one is that our proposed event-triggering condition provides a stronger assurance on the sampled-data system's performance as measured by its induced  $\mathcal{L}_2$  gain. Another important difference is that the threshold condition in equation 13 is stated in terms of the last sampled state,  $x_r$ . The corresponding threshold condition in [6] is given in terms of the current state  $x_t$ . This difference makes it easier to convert our event-triggering condition into a self-triggered feedback scheme.

## V. ADMISSIBLE RELEASE AND FINISHING TIMES

This section establishes sufficient conditions for the existence of admissible sequences of release and finishing times that ensure the sampled data system in equation 7 is  $\mathcal{L}_2$  stable with

a specified gain. These conditions take the form of admissible bounds on the task sampling periods,  $T_k$ , and task delays,  $D_k$ .

For notational convenience let  $z_k : [r_k, f_{k+1}) \rightarrow \mathfrak{R}^n$  be given as

$$z_k(t) = \sqrt{(1 - \beta^2)I + Q} = \sqrt{M}e_k(t) \quad (14)$$

where  $\sqrt{M}$  is a matrix square root and  $M$  is defined in equation 12. We refer to  $z_k$  as the  $k$ th job's "trigger signal". Note that  $M$  is dependent on the parameter  $\beta$ .

We define the function  $\rho : \mathfrak{R}^n \rightarrow \mathfrak{R}$  given by

$$\rho(x) = \sqrt{x^T M x} \quad (15)$$

where  $x \in \mathfrak{R}^n$ . So if we can guarantee for any  $\delta \in (0, 1]$  that

$$\|z_k(t)\|_2 \leq \delta \rho(x_r) \quad (16)$$

for all  $t \in [f_k, f_{k+1})$  for any  $k = 0, \dots, \infty$ , then the hypotheses in corollary 4.2 are satisfied and we can conclude that the sampled-data system is finite-gain  $\mathcal{L}_2$  stable with a gain less than  $\gamma/\beta$ .

The first major result examines what happens if we use equation 16 as the basis for an event-triggered feedback control system. In particular, let's assume that the  $k$ th job's release,  $r_k$ , is precisely that time when  $\|z_k(t)\|_2 = \delta \rho(x_r)$  under the assumption that the  $k$ th job's delay,  $D_k$ , is zero. The following theorem states a lower bound on the sampling period for which a sampled-data system with zero delay (i.e.  $D_k = 0$ ) has an induced  $\mathcal{L}_2$  gain less than  $\gamma/\beta$ .

*Theorem 5.1:* Consider the sampled-data system in equation 7 and assume there exists a non-negative real constant  $W$  such that  $\|w_t\|_2 \leq W\|x_t\|_2$  for all  $t \in \mathfrak{R}$ . Assume that for some  $\delta \in (0, 1]$  that the sequence of release times  $\{r_k\}_{k=0}^{\infty}$  satisfy

$$\|z(r_{k+1})\|_2 = \delta \rho(x_r) \quad (17)$$

where  $f_k = r_k$  for all  $k = 0, \dots, \infty$ .

The sequence of release and finishing times is admissible and the sampled-data system is  $\mathcal{L}_2$ -stable with a gain less than  $\gamma/\beta$ . Furthermore, the task sampling periods satisfy

$$T_k \geq \frac{1}{\alpha} \ln \left( 1 + \delta \alpha \frac{\rho(x_r)}{\mu_0(x_r)} \right) \quad (18)$$

where  $\alpha$  is a real constant

$$\alpha = \left\| \sqrt{M} A \sqrt{M}^{-1} \right\| + W \left\| \sqrt{M} \right\| \left\| \sqrt{M}^{-1} \right\| \quad (19)$$

and  $\mu_0 : \mathfrak{R}^n \rightarrow \mathfrak{R}$  is a real-valued function given by

$$\mu_0(x_r) = \left\| \sqrt{M} A_{cl} x_r \right\|_2 + W \left\| \sqrt{M} \right\| \|x_r\|_2. \quad (20)$$

*Proof:* The time derivative of  $\|z_k(t)\|_2$  for  $t \in [r, f^+)$  satisfies

$$\begin{aligned} \frac{d}{dt} \|z_k(t)\|_2 &\leq \left\| \sqrt{M} \dot{e}_k(t) \right\|_2 = \left\| \sqrt{M} \dot{x}_t \right\|_2 \\ &= \left\| \sqrt{M} (A x_t - B B^T P x_r + w_t) \right\|_2 \\ &\leq \left\| \sqrt{M} A e_k(t) \right\|_2 + \left\| \sqrt{M} A_{cl} x_r \right\|_2 + \left\| \sqrt{M} \right\| \|w_t\|_2 \end{aligned} \quad (21)$$

Since  $\|w_t\|_2 \leq W \|x_t\|_2$ ,  $x_t = e_k(t) + x_r$ , and  $z_k(t) = \sqrt{M} e_k(t)$ , we can bound the preceding equation (21) as

$$\begin{aligned} \frac{d}{dt} \|z_k(t)\|_2 &\leq \left\| \sqrt{M} A \sqrt{M}^{-1} \right\| \|z_k(t)\|_2 + \left\| \sqrt{M} A_{cl} x_r \right\|_2 \\ &\quad + W \left( \left\| \sqrt{M} \right\| \left\| \sqrt{M}^{-1} z_k(t) \right\|_2 + \left\| \sqrt{M} \right\| \|x_r\|_2 \right) \\ &= \left( \left\| \sqrt{M} A \sqrt{M}^{-1} \right\| + W \left\| \sqrt{M} \right\| \left\| \sqrt{M}^{-1} \right\| \right) \|z_k(t)\|_2 \\ &\quad + \left\| \sqrt{M} A_{cl} x_r \right\|_2 + W \left\| \sqrt{M} \right\| \|x_r\|_2 \\ &= \alpha \|z_k(t)\|_2 + \mu_0(x_r). \end{aligned} \quad (22)$$

where  $\alpha$  and  $\mu_0 : \mathfrak{R}^n \rightarrow \mathfrak{R}$  are defined in equations 19 and 20, respectively.

The initial condition is  $\|z_k(r)\|_2 = 0$ . Using this in the differential inequality (eq. 22) yields,

$$\|z_k(t)\|_2 \leq \frac{\mu_0(x_r)}{\alpha} \left( e^{\alpha(t-r)} - 1 \right) \quad (23)$$

for all  $t \in [r, f^+)$ .

By assumption  $r^+ = f^+$  (i.e. no task delay) and  $\delta\rho(x_r) = \|z_k(r^+)\|_2$ , so we can conclude that

$$\delta\rho(x_r) = \|z_k(r^+)\|_2 \leq \frac{\mu_0(x_r)}{\alpha} \left( e^{\alpha T_k} - 1 \right) \quad (24)$$

where  $T_k = r^+ - r$  is the task sampling period for job  $k$ . Solving equation 24 for  $T_k$  yields equation 18. The righthand side of the inequality 18 is clearly strictly greater than zero, which implies that  $r_{k+1} - r_k > 0$ . Therefore  $r_k = f_k \leq r_{k+1}$  which implies that the sequence of

finishing and release times is admissible. Finally we know that  $\|z_k(t)\|_2 \leq \delta\rho(x_r)$  for all  $t \in [r_k, f_{k+1}) = [f_k, f_{k+1})$  and all  $k = 0, \dots, \infty$ , which by corollary 4.2 implies that the system is  $\mathcal{L}_2$  stable with a gain less than  $\gamma/\beta$ . ■

*Remark 5.2:* Note that the righthand side of equation 18 will always be strictly greater than zero. We can therefore conclude that if we trigger release times when  $\delta\rho(x_r) = \|z_k(r^+)\|$ , then the sampling period  $T_k$  can never be zero.

*Remark 5.3:* The admissibility of sequences  $\{r_k\}_{k=0}^\infty$  and  $\{f_k\}_{k=0}^\infty$  can be restated in terms of the sequences  $\{D_k\}_{k=0}^\infty$  and  $\{T_k\}_{k=0}^\infty$ . By definition, the release and finishing time sequences are admissible if and only if  $r_k \leq f_k \leq r_{k+1}$  for all  $k$ . Clearly this holds if and only if  $0 \leq D_k \leq T_k$  for all  $k$ .

The previous theorem presumes there is no task delay (i.e.  $D_k = 0$ ). Under this assumption, theorem 5.1 states that triggering release times when equation 17 holds assures the closed-loop system's induced  $\mathcal{L}_2$  gain. This theorem, however, also provides a lower bound on the task sampling period, which suggests that we can also use theorem 5.1 as the basis for state-based self-triggered feedback. In this scenario, if the  $k$ th job would set the next job's release time as

$$r_{k+1} = r_k + \frac{1}{\alpha} \ln \left( 1 + \delta\alpha \frac{\rho(x_r)}{\mu_0(x_r)} \right) \quad (25)$$

then we are again assured of the system's induced  $\mathcal{L}_2$  gain is less than  $\gamma/\beta$ .

The problem faced in using equation 25 for self-triggering is the assumption of no task delay. In many application, task delay may not be small enough to neglect. If we consider non-zero delay, then the triggering signals appear as shown in figure 1. This figure shows the time history for the triggering signals,  $z_{k-1}$ ,  $z_k$ , and  $z_{k+1}$ . With non-zero delay, we can partition the time interval  $[r_k, f_{k+1})$  into two subintervals  $[r_k, f_k)$  and  $[f_k, f_{k+1})$ . The differential equations associated with subintervals  $[r_k, f_k)$  and  $[f_k, f_{k+1})$  are

$$\dot{x}(t) = Ax(t) - BB^T Px_{r^-} + w(t)$$

and

$$\dot{x}(t) = Ax(t) - BB^T Px_r + w(t),$$

respectively. In a manner similar to the proof of theorem 5.1, we can use differential inequalities to bound  $z_k(t)$  for all  $t \in [r_k, f_{k+1})$  and thereby determine sufficient conditions assuring the admissibility of the release/finishing times while preserving the closed-loop system's  $\mathcal{L}_2$ -stability.

The next two lemmas (lemma 5.4 and 5.5) characterize the behavior of  $z_k(t)$  over these two subintervals. We then use lemma 5.5 to establish sufficient conditions assuring the  $\mathcal{L}_2$ -stability of the sampled-data system with non-zero delay.

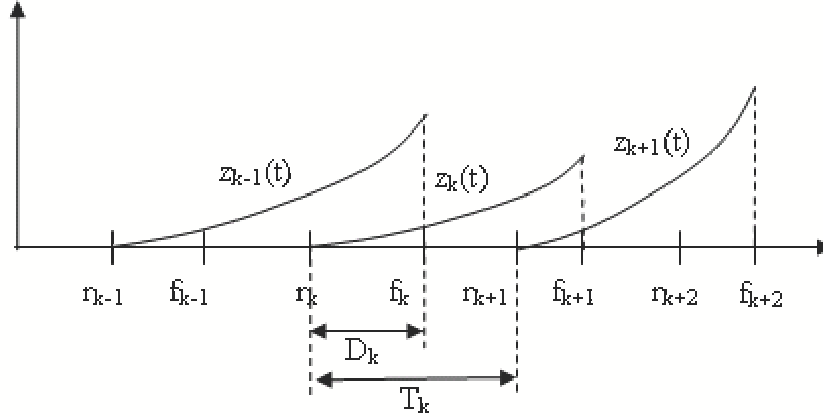


Fig. 1. Time history of  $z_k(t)$  with non-zero task delay.

*Lemma 5.4:* Consider the sampled-data system where  $\|w_t\|_2 \leq W\|x_t\|_2$  for all  $t \in \mathfrak{R}$  for some non-negative real  $W$ . Assume that for some  $k$ ,  $r_{k-1} \leq f_{k-1} \leq r_k$ . If for some  $\epsilon \in (0, 1)$ , the  $k$ th finishing time  $f_k$  satisfies

$$0 \leq D_k = f_k - r_k \leq L_1(x_r, x_{r-}; \epsilon) \quad (26)$$

for all  $t \in [r, f)$ , then the  $k$ th trigger signal,  $z_k$ , satisfies

$$\|z_k(t)\|_2 \leq \phi(x_r, x_{r-}; t - r) \leq \epsilon \rho(x_r) \quad (27)$$

for all  $t \in [r, f)$ . In equation 27  $\alpha$  is a positive real constant given by equation 19,  $L_1 : \mathfrak{R}^n \times \mathfrak{R}^n \times (0, 1) \rightarrow \mathfrak{R}$  is a real-valued function given by

$$L_1(x_r, x_{r-}; \epsilon) = \frac{1}{\alpha} \ln \left( 1 + \epsilon \alpha \frac{\rho(x_r)}{\mu_1(x_r, x_{r-})} \right), \quad (28)$$

$\phi : \mathfrak{R}^n \times \mathfrak{R}^n \times \mathfrak{R} \rightarrow \mathfrak{R}$  is a real-valued function given by

$$\phi(x_r, x_{r-}; t - r) = \frac{\mu_1(x_r, x_{r-})}{\alpha} \left( e^{\alpha(t-r)} - 1 \right), \quad (29)$$

$\rho : \mathfrak{R}^n \rightarrow \mathfrak{R}$  is given by equation 15, and  $\mu_1 : \mathfrak{R}^n \times \mathfrak{R}^n \rightarrow \mathfrak{R}$  is a real-valued function given by

$$\mu_1(x_r, x_{r-}) = \left\| \sqrt{M} \left( Ax_r - BB^T P x_{r-} \right) \right\|_2 + W \left\| \sqrt{M} \right\| \|x_r\|_2. \quad (30)$$

*Proof:* For  $t \in [r, f)$ , the derivative of  $\|z_k(t)\|_2$  satisfies the differential inequality,

$$\begin{aligned}
\frac{d}{dt}\|z_k(t)\|_2 &\leq \|\dot{z}_k(t)\|_2 = \|\sqrt{M}\dot{e}_k(t)\|_2 = \|\sqrt{M}\dot{x}(t)\|_2 \\
&= \|\sqrt{M}(Ax_t - BB^T Px_{r^-} + w_t)\|_2 \\
&= \|\sqrt{M}(Ae_k(t) + Ax_r - BB^T Px_{r^-} + w_t)\|_2 \\
&\leq \left( \|\sqrt{M}A\sqrt{M}^{-1}\| + W\|\sqrt{M}\| \|\sqrt{M}^{-1}\| \right) \|z_k(t)\|_2 \\
&\quad + \|\sqrt{M}(Ax_r - BB^T Px_{r^-})\|_2 + W\|\sqrt{M}\| \|x_r\|_2 \\
&= \alpha\|z_k(t)\|_2 + \mu_1(x_r, x_{r^-}).
\end{aligned} \tag{31}$$

The differential inequality in equation 31 along with the initial condition  $z_k(r) = 0$ , allows us to conclude that

$$\|z_k(t)\|_2 \leq \phi(x_r, x_{r^-}; t - r) \tag{32}$$

for all  $t \in [r, f)$ .

The assumption in equation 26 can be rewritten as

$$\phi(x_r, x_{r^-}; D_k) \leq \epsilon\rho(x_r) \tag{33}$$

$\phi(x_r, x_{r^-}; t - r)$  is a monotone increasing function of  $t - r$ . Combining this fact with equations 32 and 33 yields

$$\|z_k(t)\|_2 \leq \phi(x_r, x_{r^-}; t - r) \leq \phi(x_r, x_{r^-}; D_k) \leq \epsilon\rho(x_r)$$

which leads to equation 27 holding for all  $t \in [r, f)$ . ■

*Lemma 5.5:* Consider the sampled-data system in equation 7 where  $\|w_t\|_2 \leq W\|x_t\|_2$  for some non-negative real  $W$ . For a given integer  $k$  and some  $\epsilon \in (0, 1)$ , assume that  $r_{k-1} \leq f_{k-1} \leq r$ . For any  $\eta \in (\epsilon, 1]$ , let

$$d_\eta = f_k + L_2(x_r, x_{r^-}; D_k, \eta), \tag{34}$$

where  $L_2 : \mathfrak{R}^n \times \mathfrak{R}^n \times \mathfrak{R} \times (0, 1] \rightarrow \mathfrak{R}$  is given by

$$L_2(x_r, x_{r^-}; D_k, \eta) = \frac{1}{\alpha} \ln \left( 1 + \alpha \frac{\eta\rho(x_r) - \phi(x_r, x_{r^-}; D_k)}{\mu_0(x_r) + \alpha\phi(x_r, x_{r^-}; D_k)} \right). \tag{35}$$

if

$$0 \leq D_k \leq L_1(x_r, x_{r-}; \epsilon) \quad (36)$$

then

$$d_\eta > f_k, \text{ and} \quad (37)$$

$$\|z_k(t)\|_2 \leq \eta\rho(x_r) \text{ for all } t \in [f_k, d_\eta] \quad (38)$$

*Proof:* The hypotheses of this lemma also satisfy the hypotheses of lemma 5.4 so we know that

$$\|z_k(f)\|_2 \leq \phi(x_r, x_{r-}; D_k) \leq \epsilon\rho(x_r) \leq \eta\rho(x_r). \quad (39)$$

By equation 35 and 39, we have

$$L_2(x_r, x_{r-}; D_k, \eta) > 0$$

which implies

$$d_\eta > f_k$$

Assume the system state  $x_t$  satisfies the differential equation

$$\dot{x}_t = Ax_t - BB^T Px_r + w_t$$

for  $t \in [f_k, d_\eta]$ . Using an argument similar to that in lemma 5.4, we can show that  $\|z_k(t)\|_2$  satisfies the differential inequality

$$\frac{d}{dt} \|z_k(t)\|_2 \leq \alpha \|z_k(t)\|_2 + \mu_0(x_r). \quad (40)$$

Equation 39 can be viewed as an initial condition on the differential inequality in equation 40. Solving the differential inequality, we know for all  $t \in [f_k, d_\eta]$ ,

$$\|z_k(t)\|_2 \leq e^{\alpha(t-f)} \phi(x_r, x_{r-}; D_k) + \frac{\mu_0(x_r)}{\alpha} (e^{\alpha(t-f)} - 1). \quad (41)$$

Because the right side of equation 41 is an increasing function of  $t$ , we get

$$\|z_k(t)\|_2 \leq e^{\alpha(d_\eta-f)} \phi(x_r, x_{r-}; D_k) + \frac{\mu_0(x_r)}{\alpha} (e^{\alpha(d_\eta-f)} - 1) = \eta\rho(x_r). \quad (42)$$

for all  $t \in [f_k, d_\eta]$ . ■

According to lemma 5.5, for a constant  $\delta \in (\epsilon, 1)$ , if  $r^+ = f + L_2(x_r, x_{r^-}; D_k, \delta)$  and  $f^+ \leq f + L_2(x_r, x_{r^-}; D_k, 1)$ , we will always have  $\|z_k(r^+)\|_2 \leq \delta\rho(x_r)$  and  $\|z_k(f^+)\|_2 \leq \rho(x_r)$ . We will use this fact below to characterize a self-triggering scheme that preserves the sampled-data system induced  $\mathcal{L}_2$  gain. Theorem 5.7 formally states this self-triggering scheme. The proof of theorem 5.7 requires the following lemma showing that the longest allowable task delay given in lemma 5.4 is bounded below by a positive function of  $x_{r^-}$ .

*Lemma 5.6:* Consider the sampled-data system where  $\|w_t\|_2 \leq W\|x_t\|_2$  for all  $t \in \mathfrak{R}$  where  $W$  is a non-negative real constant. Assume that for a constant  $\delta \in (\epsilon, 1)$ , the release time  $r^-$  and  $r$  satisfy

$$\|z_{k-1}(r)\|_2 \leq \delta\rho(x_{r^-}) \quad (43)$$

for any given  $k$ . Then there exists a function  $\xi : \mathfrak{R}^n \times (0, 1) \times (0, 1) \rightarrow \mathfrak{R}^+$  such that the function  $L_1 : \mathfrak{R}^n \times \mathfrak{R}^n \times (0, 1) \rightarrow \mathfrak{R}$  given by equation 28 satisfies the bound

$$L_1(x_r, x_{r^-}; \epsilon) \geq \xi(x_{r^-}; \epsilon, \delta) > 0. \quad (44)$$

*Proof:* First note that  $x_r = e_{k-1}(r) + x_{r^-}$  implies that

$$\|x_{r^-}\|_2 - \|e_{k-1}(r)\|_2 \leq \|x_r\|_2 \leq \|x_{r^-}\|_2 + \|e_{k-1}(r)\|_2$$

We now use this inequality to bound  $\rho(x_r)$  and  $\mu_1(x_r, x_{r^-})$  as a function of  $x_{r^-}$ .

A lower bound on  $\rho(x_r)$  is obtained by noting that

$$\begin{aligned} \rho(x_r) &= \|\sqrt{M}x_r\|_2 = \|\sqrt{M}(e_{k-1}(r) + x_{r^-})\|_2 \\ &\geq \|\sqrt{M}x_{r^-}\|_2 - \|z_{k-1}(r)\|_2 \\ &\geq \rho(x_{r^-}) - \delta\rho(x_{r^-}) \end{aligned} \quad (45)$$

$$= (1 - \delta)\rho(x_{r^-}) \equiv \xi_1(x_{r^-}; \delta) \quad (46)$$

An upper bound on  $\mu_1(x_r, x_{r^-})$  can be obtained by noting that

$$\begin{aligned} \mu_1(x_r, x_{r^-}) &= \|\sqrt{M}(Ax_r - BB^T Px_{r^-})\|_2 + W\|\sqrt{M}\| \|x_r\|_2 \\ &= \|\sqrt{M}(A_{cl}x_{r^-} + Ae_{k-1}(r))\|_2 + W\|\sqrt{M}\| \|x_{r^-} + e_{k-1}(r)\|_2 \\ &\leq \|\sqrt{M}A_{cl}x_{r^-}\|_2 + W\|\sqrt{M}\| \|x_{r^-}\|_2 \\ &\quad + \left\| \sqrt{M}A\sqrt{M}^{-1} z_{k-1}(r) \right\|_2 + W\|\sqrt{M}\| \left\| \sqrt{M}^{-1} z_{k-1}(r) \right\|_2 \end{aligned}$$



$$\begin{aligned}
&\leq \left\| \sqrt{M} A_{\text{cl}} x_{r^-} \right\| + W \left\| \sqrt{M} \right\| \|x_{r^-}\|_2 \\
&\quad + \left( \left\| \sqrt{M} A \sqrt{M}^{-1} \right\| + W \left\| \sqrt{M} \right\| \left\| \sqrt{M}^{-1} \right\| \right) \delta \rho(x_{r^-}) \\
&= \mu_0(x_{r^-}) + \alpha \delta \rho(x_{r^-}) \equiv \xi_2(x_{r^-}; \delta)
\end{aligned} \tag{47}$$

Putting both inequalities together we see that

$$\begin{aligned}
L_1(x_r, x_{r^-}; \epsilon) &= \frac{1}{\alpha} \ln \left( 1 + \epsilon \alpha \frac{\rho(x_r)}{\mu_1(x_r, x_{r^-})} \right) \\
&\geq \frac{1}{\alpha} \ln \left( 1 + \epsilon \alpha \frac{\xi_1(x_{r^-}; \delta)}{\xi_2(x_{r^-}; \delta)} \right) \\
&= \frac{1}{\alpha} \ln \left( 1 + \epsilon \alpha \frac{(1 - \delta) \rho(x_{r^-})}{\alpha \delta \rho(x_{r^-}) + \mu_0(x_{r^-})} \right) \equiv \xi(x_{r^-}; \epsilon, \delta) > 0
\end{aligned} \tag{48}$$

which completes the proof. ■

With the preceding technical lemma we can now state a self-triggered feedback scheme which can guarantee the sampled-data system's induced  $\mathcal{L}_2$  gain. The basis for this self-triggering scheme will be found in the following theorem.

*Theorem 5.7:* Consider the sampled-data system in equation 7 where  $\|w_t\|_2 \leq W \|x_t\|_2$  for all  $t \in \mathfrak{R}^+$  where  $W$  is some non-negative real constant. For given  $\epsilon \in (0, 1)$  and  $\delta \in (\epsilon, 1)$ , we assume that

- The initial release and finishing times satisfy

$$r_{-1} = r_0 = f_0 = 0$$

- For any non-negative integer  $k$ , the release times are generated by the following recursion,

$$r_{k+1} = f_k + L_2(x(r_k), x(r_{k-1}); D_k, \delta) \tag{49}$$

and the finishing times satisfy

$$r_{k+1} \leq f_{k+1} \leq r_{k+1} + \xi(x(r_k); \epsilon, \delta). \tag{50}$$

where  $L_2$  is given in equation 35 and  $\xi$  is given in equation 48. Then the sequence of release times,  $\{r_k\}_{k=0}^\infty$ , and finishing time,  $\{f_k\}_{k=0}^\infty$ , will be admissible and the sampled-data system is finite gain  $\mathcal{L}_2$  stable with an induced gain less than  $\gamma/\beta$ .

*Proof:* From the definition of  $\xi$  in equation 48, we can easily see that  $\xi(x_r; \epsilon, \delta) > 0$  for any non-negative integer  $k$ . We can therefore use equation 50 to conclude that the interval  $[r_{k+1}, r_{k+1} + \xi(x_r; \epsilon, \delta)]$  is nonempty for all  $k$ .

Next, we insert equation 49 into equation 50 to show that

$$\begin{aligned}
f_{k+1} &\leq r_{k+1} + \xi(x(r_k); \epsilon, \delta) \\
&\leq f_k + L_2(x(r_k), x(r_{k-1}); D_k, \delta) + \xi(x(r_k)); \epsilon, \delta) \\
&= f_k + L_2(x(r_k), x(r_{k-1}); D_k, 1)
\end{aligned} \tag{51}$$

for all non-negative integers  $k$ .

With the preceding two preliminary results, we now consider the following statement about the  $k$ th job. This statement is that

- 1)  $r_k \leq f_k \leq r_{k+1}$ ,
- 2)  $\|z_k(t)\|_2 \leq \delta \rho(x(r_k))$  for all  $t \in [f_k, r_{k+1}]$ ,
- 3) and  $\|z_k(t)\|_2 \leq \rho(x(r_k))$  for all  $t \in [f_k, f_{k+1}]$ .

We now use mathematical induction to show that under the theorem's hypotheses, this statement holds for all non-negative integers  $k$ .

First consider the base case when  $k = 0$ . According to the definition of  $L_2$  (equation 35) we know that

$$L_2(x_0, x_0; D_0, \delta) = L_2(x_0, x_0; D_k, \delta) > 0$$

We can therefore combine equations 50 and 49 to obtain

$$r_0 = f_0 \leq f_0 + L_2(x_0, x_0; D_0, \delta) = r_1 \tag{52}$$

which establishes the first part of the inductive statement when  $k = 0$ .

Next note that

$$D_0 = 0 \leq L_1(x(r_0), x(r_{-1}); \epsilon). \tag{53}$$

If we use the fact that  $\delta \in (\epsilon, 1) \subset (0, 1]$  in equations 49 and 53, we can see that the hypotheses of lemma 5.5 are satisfied. This means that  $\|z_0(t)\|_2 \leq \delta \rho(x(r_0))$  for all  $t \in [f_0, r_1]$  which completes the second part of the inductive statement for  $k = 0$ .

Now define the time

$$d_1^0 = f_0 + L_2(x(r_0), x(r_{-1}); D_0, 1)$$

Equation 53 again implies that the hypotheses of lemma 5.5 are satisfied, so that

$$\|z_0(t)\|_2 \leq \rho(x(r_0)) \text{ for all } t \in [f_0, d_1^0]. \tag{54}$$

From equation 51, we know that  $f_1 \leq d_1^0$ . We can also combine equations 50 and 52 to conclude that  $f_0 \leq f_1$ . We therefore know that  $[f_0, f_1] \subseteq [f_1, d_1^0]$  which combined with equation 54 implies that

$$\|z_0(t)\|_2 \leq \rho(x(r_0)) \text{ for all } t \in [f_1, d_1^0]$$

This therefore establishes the last part of the inductive statement for  $k = 0$ .

We now turn to the general case for any  $k$ . For a given  $k$  let's assume that the statement holds. This means that

$$r_k \leq f_k \leq r_{k+1} \tag{55}$$

$$\|z_k(t)\|_2 \leq \delta\rho(x(r_k)) \text{ for all } t \in [f_k, r_{k+1}] \tag{56}$$

$$\|z_k(t)\|_2 \leq \rho(x(r_k)) \text{ for all } t \in [f_k, f_{k+1}] \tag{57}$$

Now consider the  $k + 1$ st job. Because equation 56 is true, the hypothesis of lemma 5.6 is satisfied which means there exists a function  $\xi$  (given by equation 48) such that

$$0 < \xi(x(r_k)); \epsilon, \delta \leq L_1(x(r_{k+1}), x(r_k); \epsilon).$$

We can use this in equation 50 to obtain

$$0 \leq D_{k+1} = f_{k+1} - r_{k+1} \leq \xi(x(r_k); \epsilon, \delta) \leq L_1(x(r_{k+1}), x(r_k); \epsilon). \tag{58}$$

From equation 58 and the fact that  $\delta \in (0, 1)$  we know that the hypotheses of lemma 5.5 hold and we can conclude that

$$f_{k+1} \leq r_{k+2} \tag{59}$$

$$\|z_{k+1}\|_2 \leq \delta\rho(x(r_{k+1})) \text{ for all } t \in [f_{k+1}, r_{k+2}]. \tag{60}$$

Combining equation 50 with the above equation 59 yields  $r_{k+1} \leq f_{k+1} \leq r_{k+2}$  which establishes the first part of the statement for the case  $k + 1$ . Equation 60 is the second part of the statement.

Finally let

$$d_1^{k+1} = f_{k+1} + L_2(x(r_{k+1}), x(r_k); D_{k+1}, 1)$$

Following our prior argument for the case when  $k = 0$ , we know that the validity of equation 58 satisfies the hypotheses of lemma 5.5. We can therefore conclude that

$$\|z_{k+1}(t)\|_2 \leq \rho(x(r_{k+1})) \text{ for all } t \in [f_{k+1}, d_1^{k+1}] \tag{61}$$

According to equation 51,  $f_{k+2} \leq d_1^{k+1}$ . We can therefore combine equations 50 and 59 to show that  $f_{k+1} \leq f_{k+2}$  and therefore conclude that  $[f_{k+1}, f_{k+2}] \subseteq [f_{k+1}, d_1^{k+1}]$ . Combining this observation with equation 61 yields  $\|z_{k+1}(t)\|_2 \leq \rho(x(r_{k+1}))$  for all  $t \in [f_{k+1}, f_{k+2}]$  which completes the third part of the inductive statement for case  $k + 1$ .

We may therefore use mathematical induction to conclude that the inductive statement holds for all non-negative integers  $k$ . The first part of the statement, of course, simply means that the sequences  $\{r_k\}_{k=0}^\infty$  and  $\{f_k\}_{k=0}^\infty$  are admissible. The third part of the inductive statement implies that the hypotheses of corollary 4.2 are satisfied, thereby ensuring that the system's induced  $\mathcal{L}_2$  gain is less than  $\gamma/\beta$ . ■

*Remark 5.8:*  $\xi(x_r; \epsilon, \delta)$  serves as the deadline for the delay  $D_k$  in theorem 5.7.

*Remark 5.9:* By the way we constructed  $\delta$ , we see that it controls when the next job's finishing time. We might therefore expect to see a larger  $\delta$  result in larger sampling periods. This is indeed confirmed by the analysis. Since

$$T_k \geq r_{k+1} - f_k = L_2(x_r, x_{r-}; D_k, \delta)$$

and since  $L_2$  is an increasing function of  $\delta$  we can see that larger  $\delta$  result in larger sampling periods.

*Remark 5.10:* By our construction of the parameter  $\epsilon$ , we see that it controls the current job's finishing time. Since this

$$D_k = f_k - r_k \leq \xi(x_r; \epsilon, \delta)$$

and since  $\xi$  is an increasing function of  $\epsilon$ , we can expect to see the allowable delay increase as we increase  $\epsilon$ . Note also that  $\xi$  is a decreasing function of  $\delta$  so that adopting a longer sampling period by increasing  $\delta$  will have the effect of reducing the maximum allowable task delay.

The following corollary to the above theorem shows that the task periods and deadlines generated by our self-triggered scheme are all bounded away from zero. This is important in establishing that our scheme does not generate infinite sampling frequencies.

*Corollary 5.11:* Assume the assumptions in theorem 5.7 hold. Then there exist two positive constants  $\zeta_1, \zeta_2 > 0$  such that

$$T_k \geq \zeta_1$$

and

$$\xi(x_r; \epsilon, \delta) \geq \zeta_2$$

*Proof:* From theorem 5.7, we know

$$f_k - r_k \leq \xi(x_r; \epsilon, \delta) \leq L_1(x_r, x_{r-}; \epsilon)$$

Therefore, by lemma 5.4,

$$\|z_k(f)\|_2 \leq \phi(x_r, x_{r-}; D_k) \leq \epsilon \rho(x_r)$$

Let us first take a look at  $T_k$ . From equation 49, we have

$$\begin{aligned} T_k &\geq r_{k+1} - f_k \\ &= L_2(x_r, x_{r-}; D_k, \delta) \\ &= \frac{1}{\alpha} \ln \left( 1 + \alpha \frac{\delta \rho(x_r) - \phi(x_r, x_{r-}; D_k)}{\mu_0(x_r) + \alpha \phi(x_r, x_{r-}; D_k)} \right) \\ &\geq \frac{1}{\alpha} \ln \left( 1 + \alpha \frac{\delta \rho(x_r) - \epsilon \rho(x_r)}{\mu_0(x_r) + \alpha \epsilon \rho(x_r)} \right) \\ &\geq \frac{1}{\alpha} \ln \left( 1 + \alpha \frac{(\delta - \epsilon) \underline{\lambda}(\sqrt{M}) \|x_r\|_2}{\|\sqrt{M} A_{cl}\| \|x_r\|_2 + W \|\sqrt{M}\| \|x_r\|_2 + \alpha \epsilon \bar{\lambda}(\sqrt{M}) \|x_r\|_2} \right) \\ &= \frac{1}{\alpha} \ln \left( 1 + \alpha \frac{(\delta - \epsilon) \underline{\lambda}(\sqrt{M})}{\|\sqrt{M} A_{cl}\| + W \|\sqrt{M}\| + \alpha \epsilon \bar{\lambda}(\sqrt{M})} \right) \\ &= \zeta_1 > 0 \end{aligned} \tag{62}$$

It is easy to show that

$$\xi(x_r; \epsilon, \delta) \geq \frac{1}{\alpha} \ln \left( 1 + \frac{\epsilon \alpha (1 - \delta) \underline{\lambda}(\sqrt{M})}{\|\sqrt{M} A_{cl}\| + W \|\sqrt{M}\| + \delta \alpha \bar{\lambda}(\sqrt{M})} \right) = \zeta_2 > 0$$

■

## VI. SIMULATION

The following simulation results were generated for event-triggered and self-triggered feedback systems. The plant was an inverted pendulum on top of a moving cart. The plant's linearized state equations were

$$\dot{x}(t) = \begin{bmatrix} 0 & 1 & 0 & 0 \\ 0 & 0 & -mg/M & 0 \\ 0 & 0 & 0 & 1 \\ 0 & 0 & g/\ell & 0 \end{bmatrix} x(t) + \begin{bmatrix} 0 \\ 1/M \\ 0 \\ -1/(M\ell) \end{bmatrix} u(t) + \begin{bmatrix} 1 \\ 0 \\ 1 \\ 0 \end{bmatrix} w(t)$$

where  $M$  was the cart mass,  $m$  was the mass of the pendulum bob,  $\ell$  was the length of the pendulum arm, and  $g$  was gravitational acceleration. For these simulations, we let  $M = 10$ ,  $\ell = 3$ , and  $g = 10$ . The system state was the vector  $x = \begin{bmatrix} y & \dot{y} & \theta & \dot{\theta} \end{bmatrix}^T$  where  $y$  was the cart's position and  $\theta$  was the pendulum bob's angle with respect to the vertical. The control input  $u(t)$  was generated by either an event-triggered or self-triggered controller. The function  $w$  was an external disturbance to the system. The system's initial state was the vector  $x_0 = \begin{bmatrix} 0.98 & 0 & 0.2 & 0 \end{bmatrix}^T$ .

We designed a continuous-time state feedback control system (equation 1) in which the performance level,  $\gamma$ , was set to 200. Solving the Riccati equation in equation 2 yielded a positive definite matrix  $P$  such that the state-feedback gains were

$$B^T P = \begin{bmatrix} -2 & -12 & -378 & -210 \end{bmatrix}.$$

The state trajectory of the resulting closed-loop system is denoted below as  $x_c$ . Figure 2 plots the system states as a function of time under the assumption that  $w(t) = 0$  for all  $t$ . Figure 2 is therefore the impulse response of the inverted pendulum system.

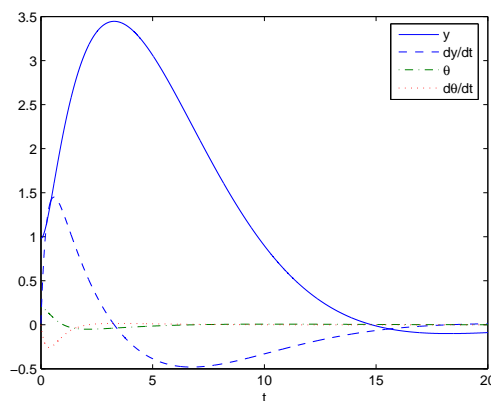


Fig. 2. State Trajectories of Continuous-time Closed-loop System (eq. 1)

### A. Event-triggered Feedback

This subsection presents simulation results for an event-triggered control of the inverted pendulum. In this simulation, the next release (after release  $r$ ) was triggered when  $\|z_k(t)\|^2 = \delta\rho(x_r)$  where  $\delta$  was set to 0.7. Recall that the trigger signal,  $z_k$ , is dependent on a parameter  $\beta$  (see equation 14). For all of the following simulations we let  $\beta = 0.5$ . The task delays were set

equal to the deadline predicted in equation 48. In other words  $D_k = \xi(x(r_{k-1}; \epsilon, \delta)) > 0$  where  $\epsilon$  was chosen to be 0.65. The external disturbance in this simulation was set to zero (i.e.  $w(t) = 0$  for all  $t$ ).

Let  $x(t)$  denote the event-triggered system's response at time  $t$ . Let  $x_c(t)$  denote the continuous-time control system's state. Figure 3 plots the error signal  $\|x(t) - x_c(t)\|_2$  as a function of time. This plot, therefore shows the difference between the event-triggered system and the original continuous-time closed loop system. The error signal is small over time, thereby suggesting that the continuous-time and event-triggered systems have nearly identical impulse responses.

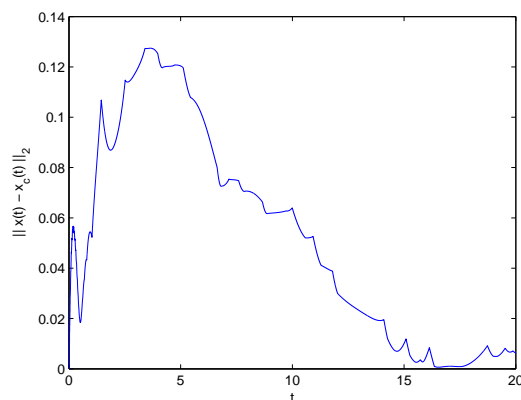


Fig. 3. State Error ( $\|x(t) - x_c(t)\|_2$ ) versus time for an event-triggered control system ( $\delta = 0.7$ ,  $\epsilon = 0.65$ ,  $w(t) = 0$ )

Figure 4 plots the task periods,  $T_k$ , (crosses) and deadlines,  $\xi$ , (dots) generated by the event-triggering scheme. The plot shows that the sampling periods generated by event-triggering range from 0.023 to 2.368 seconds with an average period of 0.349 seconds. This is a very wide range and indeed supports the assertion that event-triggering can substantially reduce the sampling frequency without adversely effecting system performance.

It is instructive to compare the sampling periods in figure 4 against the periods that would have been generated by the event-triggering scheme in [6]. The event-triggering scheme in [6] samples the state when

$$e_k^T(t) P e_k(t) = p x^T(t) P x(t).$$

$P$  is a positive definite matrix associated with a control Lyapunov function  $V(x) = x^T P x$  for the closed loop system with state feedback gains  $K$ . Since  $V$  is a control Lyapunov function,

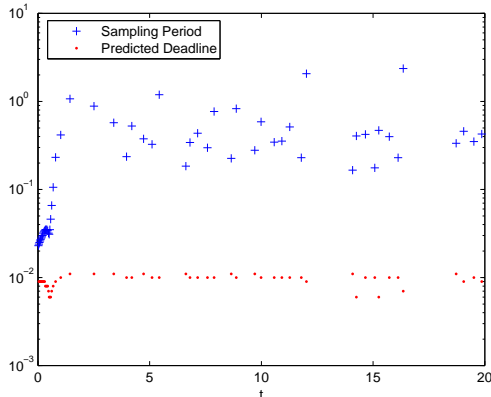


Fig. 4. Sampling periods and deadlines generated by event-triggered feedback ( $\delta = 0.7$ ,  $\epsilon = 0.65$ , and  $w(t) = 0$ )

we can find a matrix  $H$  such that the directional derivative of the unforced closed loop system satisfies the inequality  $\dot{V} \leq -x^T H x$ . In the above equation,  $p$  is the real constant

$$p = \frac{\lambda_m(P)}{2\lambda_M(P)} \frac{\lambda_m(H)}{\|PBK\|}$$

where  $\lambda_m(P)$  and  $\lambda_M(P)$  denote the minimum and maximum eigenvalues of matrix  $P$ , respectively. For this particular simulation, we used the  $P$  associated with our controller to obtain  $p = 4.17 \times 10^{-11}$ . This event-triggering threshold generates sampling periods between  $10^{-6}$  and  $10^{-4}$  seconds. This is much smaller than the sampling periods generated by event-triggering using the threshold condition in corollary 4.2. The reason for this difference is that the condition number of our  $P$  matrix is extremely large due to the great difference in the time constants associated with the dynamics of the cart and pendulum bob.

### B. Self-triggered Feedback

The simulations in this subsection examined the self-triggering feedback scheme associated with equations 49 and 50 in theorem 5.7. In this case the task release times were generated at time  $f_k$  using the equation

$$r_{k+1} = f_k + L_2(x(r_k), x(r_{k-1}), D_k, \delta)$$

and the finishing times were required to satisfy

$$f_{k+1} = f_k + \xi(x(r_k); \epsilon, \delta)$$



We again controlled the inverted pendulum plant of the preceding subsection in which the external disturbance  $w$  was again zero. The  $\epsilon$  and  $\delta$  parameters were the same as in the preceding subsection taking values 0.65 and 0.7, respectively.

Let  $x(t)$  denote the self-triggered system's response and  $x_c$  the continuous-time system's response. Figure 5 plots the error signal  $\|x(t) - x_c(t)\|_2$  as a function of time. The error signal is again small over time, thereby suggesting that the continuous-time and self-triggered systems have nearly identical impulse responses

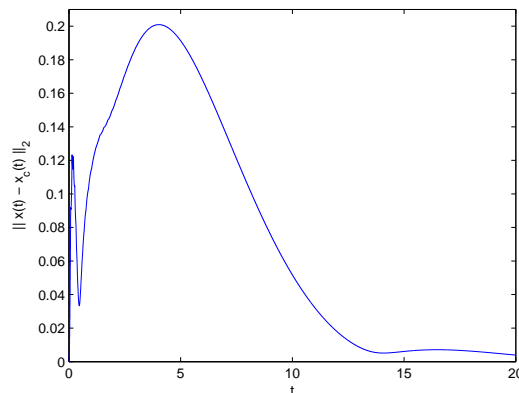


Fig. 5. State error ( $\|x(t) - x_c(t)\|_2$ ) versus time for a self-triggered control system ( $\delta = 0.7$ ,  $\epsilon = 0.65$ ,  $w(t) = 0$ ).

Figure 6 plots the task periods,  $T_k$ , (crosses) and deadlines,  $\xi$ , (dots) generated by the self-triggered scheme. The sampling periods range between 0.027 to 0.187. This is an order of magnitude lower than the periods generated by the event-triggered scheme in the preceding subsection. These sampling periods, however, still show significant variability. The shortest and most aggressive sampling periods occurred in response to the system's non-zero initial condition. Longer and relatively constant sampling periods were generated once the system state has returned to the neighborhood of the system's equilibrium point. This seems to confirm the conjecture that self-triggering can effectively adjust task periods in response to changes in the control system's external inputs.

Figures 7 and 8 show what happens to task periods and deadlines when we varied  $\delta$  and  $\epsilon$ . In figure 7,  $\delta = 0.7$  and  $\epsilon$  was varied between 0.1, 0.4 and 0.65. The top two plots show histograms of the sampling period (left) and deadline (right) for  $\epsilon = 0.65$ . The middle two plots are histograms of the sampling periods and deadlines for  $\epsilon = 0.4$ . The bottom two plots display

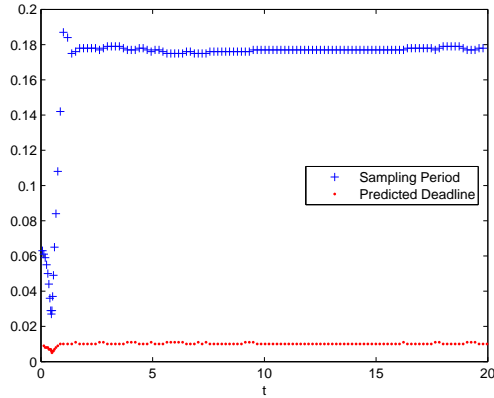


Fig. 6. Sampling period and predicted deadline for a self-triggered system in which  $\delta = 0.7$  and  $\epsilon = 0.65$ .

results when  $\epsilon = 0.1$ . Examining the three histograms on the left side of figure 7 shows little change in sampling period as a function of  $\epsilon$ . The three histograms on the right side of figure 7 show significant variation in deadline as a function of  $\epsilon$ . These results are consistent with our earlier discussion in remark 5.10. Recall that  $\epsilon$  controls the time when the  $k$ th task finishes. So by changing  $\epsilon$  we expect to see a large impact on the predicted deadline ( $\xi$ ) and little impact on the task period.

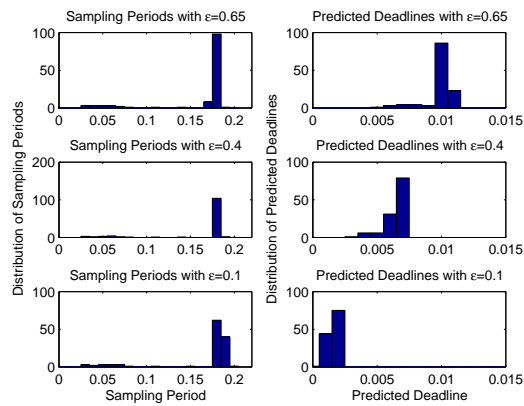


Fig. 7. Histogram of sample period and predicted deadline for a self-triggered system in which  $\delta = 0.7$  and  $\epsilon \in \{0.1, 0.4, 0.65\}$ .

Figure 8 is similar to figure 7 except that we keep  $\epsilon$  fixed at 0.1 and vary  $\delta$  from 0.15 (bottom) to 0.4 (middle) to 0.9 (top). These histograms show that as we increase  $\delta$  we also

enlarge the task periods. Recall that  $\delta$  controls the time interval  $f_{k+1} - f_k$  so that what we observe in the simulation is again consistent with our comments in remark 5.9. As we increase the sampling period, however, we can expect smaller predicted deadlines because the average sampling frequency is lower. This too is seen in the histograms on the righthand side of figure 8.

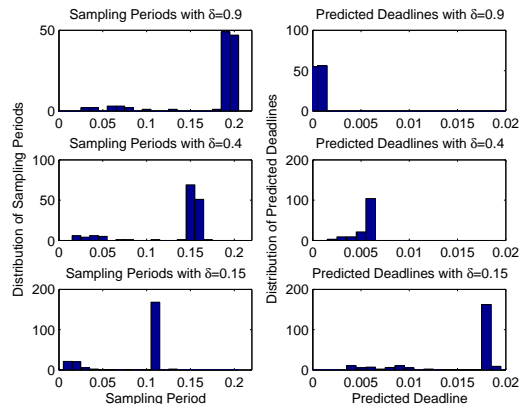


Fig. 8. Histogram of sample period and predicted deadline for a self-triggered system in which  $\epsilon = 0.1$  and  $\delta \in \{0.15, 0.40, 0.9\}$ .

The results in this subsection clearly show that we can effectively bound the task periods and deadlines in a way that preserves the closed loop system's  $\mathcal{L}_2$  stability. An interesting future research topic concerns how we might use these bounds on period and deadline in a systematic manner to schedule multiple real-time control tasks.

### C. Self-triggered versus Periodically Triggered Control

The simulations in this subsection directly compare the performance of self-triggered and "comparable" periodically triggered feedback control systems. These simulations were done on the inverted pendulum system described above. The self-triggered simulations assumed that  $\epsilon = 0.65$  and  $\delta = 0.7$  and task delays were set equal to the deadlines given by the function  $\xi$ .

The state trajectories were compared against periodically triggered systems with a *comparable* task period and delays. The comparable task periods were chosen from the sample periods generated by a self-triggered system whose exogenous inputs were chosen to be a noise process in which  $\|w(t)\|_2 \leq 0.01\|x(t)\|_2$ . The delay was set equal to the minimum predicted deadline.

Figure 9 plots the sample periods,  $T_k$ , and predicted deadlines generated by such a self-triggered system. After the initial transient in response to the system's non-zero initial condition, the sampling periods converge onto a periodic signal in which the sample periods range between 0.055 to 0.104. The mean sample period over the interval when the system is near its equilibrium point is taken as the "comparable" period for a periodically triggered control system. This comparable period was 0.0673. The comparable delay was set to the minimum predicted deadline which was 0.004.

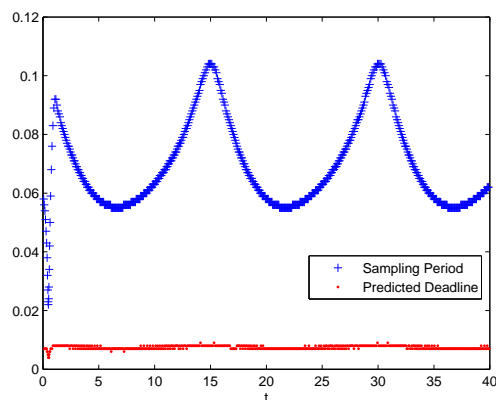


Fig. 9. Sample periods generated by a self-triggered system ( $\epsilon = 0.65$  and  $\delta = 0.7$ ) driven by a noise process.

It is interesting to note that  $T_k$  shows significant periodic variation in figure 9. Other simulations have shown similar results. These observations suggest that the choice of "optimal" sampling period has its own dynamic that leads to a period variation in the sampling periods. One interesting issue for future research is whether or not we can take advantage of this variability in the scheduling of multiple real-time control tasks.

We compared the self-triggered and periodically triggered system's performance by examining their normalized state errors,  $E(t)$ , given by

$$E(t) = \frac{|V(x(t)) - V(x_c(t))|}{V(x_c(t))}$$

where  $V(x) = x^T P x$  and  $P$  is the positive definite matrix satisfying the algebraic Riccati equation 2. This normalization of the state error allows us to fairly compare those states (i.e. the pendulum bob angle) that are most directly affected by input disturbances. The results from this comparison are shown in figure 10. This figure plots the time history of the normalized error,

$E(t)$ , for the inverted pendulum using the input signal,  $w(t) = \mu(t) + \nu(t)$  where  $\nu$  is a white noise process such that  $\|\nu(t)\|_2 \leq 0.01\|x(t)\|_2$  and  $\mu : \mathfrak{R} \rightarrow \mathfrak{R}$  takes the values

$$\mu(t) = \begin{cases} \text{sgn}(\sin(0.7t)) & \text{if } 0 \leq t < 10 \\ 0 & \text{otherwise} \end{cases}.$$

The function  $\mu$  is a square wave input to the system that we'll use to see how the self-triggered and periodically triggered systems react to external disturbances. The figure plots the normalized error for the self-triggered system and a comparable periodically triggered system. As noted above the period for the periodically-triggered system was chosen from the "steady-state" sample periods generated by the self-triggered system (see figure 9).

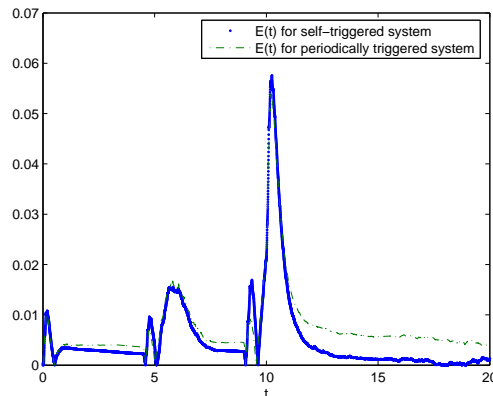


Fig. 10. Normalized error,  $E(t)$ , versus time for a self-triggered system ( $\epsilon = .65$  and  $\delta = 0.7$ ) and a periodically triggered system whose period was chosen from the sample periods shown in figure 9.

Figure 10 clearly shows that the self-triggered error is significantly smaller than the error of the periodically triggered system. This error is a direct result of the self-triggered system's ability to adjust its sample period. Figure 11 plots the sampling periods generated by the self-triggered system for the preceding system. This plot shows that the sampling period readjusts and gets smaller when the square wave input hits the system over the time interval  $[0, 10]$ . These results again demonstrate the ability of self-triggering to successfully adapt to changes in the system's input disturbances.

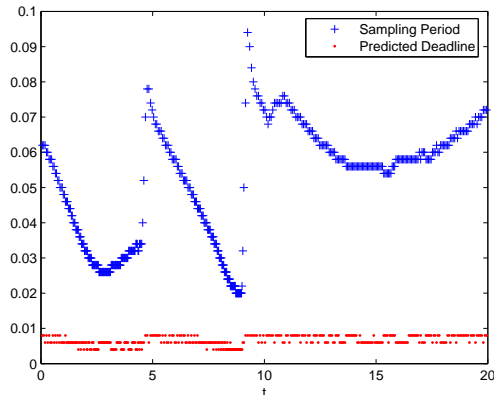


Fig. 11. Sampling period versus time for the self-triggered system ( $\epsilon = 0.65$  and  $\delta = 0.7$ ) with a square wave input over the time interval  $[0, 10]$ .

## VII. CONCLUSION

This paper has presented a state-dependent threshold inequality whose satisfaction assures the induced  $\mathcal{L}_2$  gain of a sampled-data linear state feedback control system. We derive state-dependent bounds on the task periods and deadlines enforcing this threshold inequality. These results were used to present an event-triggered feedback scheme and self-triggered feedback scheme with guaranteed  $\mathcal{L}_2$  stability. Simulation results show that the proposed event and self-triggered feedback schemes perform better than comparable periodically triggered feedback controllers. The results in this paper, therefore, appear to provide a solid analytical basis for the development of aperiodic sampled-data control systems that adjust their periods and deadlines to variations in the system's external inputs.

There are a number of open directions for future study. The bounds derived in this paper can be thought of as quality-of-control (QoC) constraint that a real-time scheduler must enforce to assure the application's (i.e. control system's) performance level. This may be beneficial in the development of soft real-time systems for controlling multiple plants. The bounds on task period and deadline suggest that real-time engineers can adjust both task period and task deadline to assure task set schedulability while meeting application performance requirements. It would be interesting to see whether such bounds can be used in generalizations of elastic scheduling algorithms [16] [17]. This might allow us to finally build soft real-time systems

providing guarantees on application performance that have traditionally been found only in hard real-time control systems.

To our best knowledge, this is the first rigorous examination of what might be required to implement self-triggered feedback control systems. Self-triggering on single processor systems may not be very useful since event-triggers can often be implemented in an inexpensive manner using programmable gate arrays (FPGA) or custom analog integrated circuits (ASIC). If, however, we are controlling multiple plants over a wireless network, then the inability of such networks to provide deterministic guarantees on message delivery make the use of self-triggered feedback much more attractive. An interesting future research direction would explore the use of self-triggered feedback over wireless sensor-actuator networks.

## REFERENCES

- [1] M. Lemmon, T. Chantem, X. Hu, and M. Zyskowski, "On self-triggered full information h-infinity controllers," in *Hybrid Systems: computation and control*, 2007.
- [2] M. Velasco, P. Marti, and J. Fuertes, "The self triggered task model for real-time control systems," in *Work-in-Progress Session of the 24th IEEE Real-Time Systems Symposium (RTSS03)*, 2003.
- [3] K. Astrom and B. Wittenmark, *Computer-Controlled Systems: theory and design*, 2nd ed. Prentice-Hall, 1990.
- [4] Y. Zheng, D. Owens, and S. Billings, "Fast sampling and stability of nonlinear sampled-data systems: Part 2. sampling rate estimations," *IMA Journal of Mathematical Control and Information*, vol. 7, pp. 13–33, 1990.
- [5] D. Netic, A. Teel, and E. Sontag, "Formulas relating kl stability estimates of discrete-time and sampled-data nonlinear systems," *Systems and Control Letters*, vol. 38, pp. 49–60, 1999.
- [6] P. Tabuada and X. Wang, "Preliminary results on state-triggered scheduling of stabilizing control tasks," in *IEEE Conference on Decision and Control*, 2006.
- [7] D. Seto, J. Lehoczky, L. Sha, and K. Shin, "On task schedulability in real-time control systems," in *IEEE Real-time Technology and Applications Symposium (RTAS)*, 1996, pp. 13–21.
- [8] A. Cervin, J. Eker, B. Bernhardsson, and K.-E. Arzen, "Feedback-feedforward scheduling of control tasks," *Real-time Systems*, vol. 23(1-2), pp. 25–53, 2002.
- [9] P. Marti, C. Lin, S. Brandt, M. Velasco, and J. Fuertes, "Optimal state feedback resource allocation for resource-constrained control tasks," in *IEEE Real-Time Systems Symposium (RTSS 2004)*, 2004, p. 161172.
- [10] B. Bamieh, "Intersample and finite wordlength effects in sampled-data problems," *IEEE Transactions on Automatic Control*, vol. 48, no. 4, pp. 639–643, 2003.
- [11] C. Liu and J. Layland, "Scheduling for multiprogramming in a hard-real-time environment," *Journal of the Association for Computing Machinery*, vol. 20, no. 1, pp. 46–61, 1973.
- [12] K. Arzen, "A simple event-based PID controller," in *Proceedings of the 14th IFAC World Congress*, 1999.
- [13] D. Hristu-Varsakelis and P. Kumar, "Interrupt-based feedback control over a shared communication medium," in *Proceedings of the IEEE Conference on Decision and Control*, 2002.

- [14] K. Astrom and B. Bernhardsson, "Comparison of riemann and lebesgue sampling for first order stochastic systems," in *Proceedings of the IEEE Conference on Decision and Control*, 1999.
- [15] P. Voulgaris, "Control of asynchronous sampled data systems," *IEEE Transactions on Automatic Control*, vol. 39, no. 7, pp. 1451–1455, 1994.
- [16] G. Buttazzo, G. Lipari, M. Caccamo, and L. Abeni, "Elastic scheduling for flexible workload management," *IEEE Transactions on Computers*, vol. 51(3), pp. 289–302, 2002.
- [17] T. Chantem, X. Hu, and M. Lemmon, "Generalized elastic scheduling," in *IEEE Real Time Systems Symposium*, 2006.